

ANALYSIS AND SIMULATION OF DETERMINISTIC CHAOS IN THE DYNAMICAL MODEL OF AEROPLANE ENGINE MOUNTING

Marian Jeż¹, Andrzej Stefański², Krzysztof Czołczyński²

¹Institute of Aeronautics,

Al. Krakowska 110, 02-250 Warszawa, Poland

²Division of Dynamics, Technical University of Łódź,
ul. Stefanowskiego 1/15, 90-924 Łódź, Poland

Abstract

A dynamic model of a piston engine mounted in the aeroplane has been formulated. The equations of motion have been identified for 4-cylinder boxer Franklin installed in the Polish aerobatic Koliber plane. Comparison of engine body acceleration RMS values obtained by measurement and simulation has given positive results. The engine body vibrations in the plane of the reactive torque of forces have been investigated in the Matlab-Simulink environment and with the help of the INSITE software. It has revealed relationships of system responses to its parameters and excitation values to assure a methodical approach to the suspension synthesis. The asymptotic methods have given multidimensional expressions for natural frequencies and resonance curves. The numerical methods have been applied to establish stability boundaries, chaos occurrence, routes to chaos and to identify chaos symptoms.

1. Introduction.

The subject of this study are vibrations of a piston engine mounted in the aerobatic plane. The aim of the study is to define suspension dynamic properties in relation to the suspension elasto-damping parameters. The diagnosis and isolation of aeroengine rubber mountings were investigated by Carr et al [1], Jeż [2], Swanson et al [10] and many other researches.

During its operation a boxer engine generates dynamic loading applied to the plane and is submitted to kinematic loading created by aeroplane aerobatics. The former one is customarily treated as determined, and the latter one – as stochastic and neglected here, because its frequency is distinctly lower than the engine proper frequency spectrum. From the piston engine investigations we know that its main excitation is the torque of forces acting in the plane perpendicular to the crankshaft axis and transmitted to the aeroplane structure by a set of several rubber mountings.

Recent investigations carried out by Moon [6], Kapitaniak [3,4], Schuster [9] and other show that chaotic behavior in nonlinear systems can be encountered by means of numerical simulation. In the present study of dynamic behavior of the aeroengine, the chaotic symptoms were identified during its operation at very small RPM with very small suspension stiffness.

2. Mathematical model formulation and identification.

The physical model shown in Figure 1 contains the independent horizontal displacement y and two linked movements: the vertical displacement z and the rotation φ . The suspension of this plane model comprises three rubber mountings: two of them transmit forces only in the direction of z axis and the third one – only in the direction of y axis.

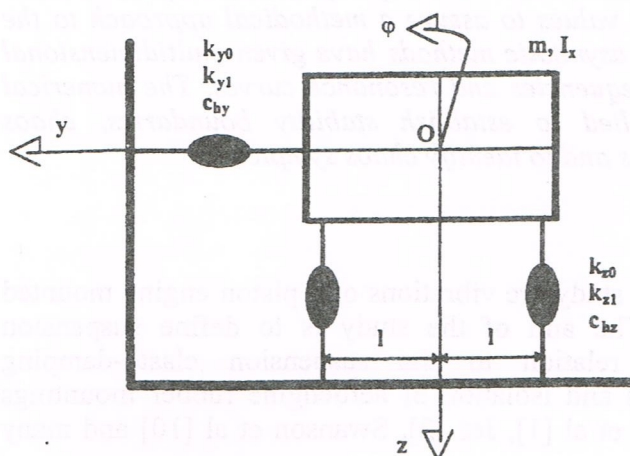


Figure 1.
The physical
model of the
engine
suspension in the
plane of
excitation.

The following differential type constitutive relations have been elaborated:

$$\ddot{\zeta} + 2 \frac{k_{z0}}{m} \dot{\zeta} = - \frac{k_{z1} l^2}{m} [(\zeta + \varphi)^3 + (\zeta - \varphi)^3] + \frac{R(\zeta, \dot{\zeta})}{m} \quad (1)$$

$$\ddot{\varphi} + 2 \frac{k_{z0} l^2}{I_x} \dot{\varphi} = - \frac{k_{z1} l^4}{I_x} [(\zeta + \varphi)^3 - (\zeta - \varphi)^3] + \frac{R(\varphi, \dot{\varphi})}{I_x} + \frac{L(t)}{I_x} \quad (2)$$

$$\ddot{v} + \frac{k_{y0}}{m} \dot{v} = - \frac{k_{y1} l^2 v^3}{m} + \frac{R(v, \dot{v})}{m}, \quad (3)$$

where:

$\zeta = z/l$, $v = y/l$ – normalised co-ordinates,
 m , I_x – system mass parameters,
 k_{y0} , k_{z0} – coefficients of linear stiffness,
 k_{y1} , k_{z1} – coefficients of nonlinear stiffness.

Excitation and damping torques are expressed by the formulas:

$$L(t) = \sum_{i=1}^{j=6} \frac{L_i}{I_x} \cos(2i\omega t + v_i) \quad (4)$$

$$R(\zeta, \dot{\zeta}) = c_{hy} |\dot{\zeta}| \text{sign}(\dot{\zeta}) \quad (5)$$

where:

L_i – amplitude of excitation,
 c_{hy} – coefficient of hysteretic damping,
 v_i – phase angle,
 ω – frequency of excitation.

The time diagram (Figure 2) and components of the exciting torque have been determined by means of measurements and customised programs.

The coefficients of nonlinear, progressive stiffness and hysteretic damping have been found with the patented method of rubber mounts dynamical identification [2].

Equation (3) describes damped vibrations aiming at the equilibrium position. So, in our computations we have considered the two-degree-of-freedom system given by equations (1) and (2). In the numerical analysis we have also taken the linear viscous damping (coefficient c) as a substitute of the hysteretic damping.

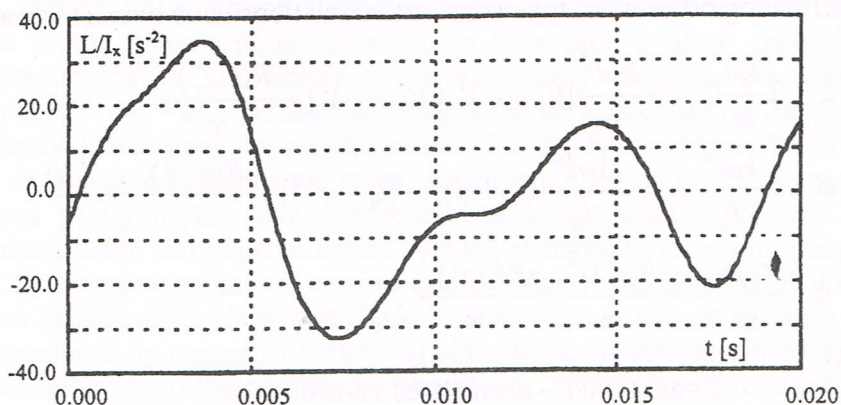


Figure 2. The time diagram of the exciting torque in engine cycle.

Taking into account parametric, dynamical identification and substitutional, linear damping, we can rewrite the model in the form of the first order differential equation, suitable for applying numerical methods of analysis:

$$\dot{\zeta}_1 = \zeta_2 \quad (6a)$$

$$\dot{\zeta}_2 = -2 \frac{k_{z0}}{m} \zeta_1 - \frac{k_{z1} l^2}{m} [(\zeta_1 + \varphi_1)^3 + (\zeta_1 - \varphi_1)^3] - \frac{c}{m} \zeta_2 \quad (6b)$$

$$\dot{\varphi}_1 = \varphi_2 \quad (7a)$$

$$\begin{aligned} \dot{\varphi}_2 = & -2 \frac{k_{z0} l^2}{I_x} \varphi_1 - \frac{k_{z1} l^4}{I_x} [(\zeta_1 + \varphi_1)^3 - (\zeta_1 - \varphi_1)^3] - \frac{cl^2}{I_x} \varphi_2 \\ & + \sum_{i=1}^{j=6} \frac{L_i}{I_x} \cos(2i\omega t + \nu_i) \end{aligned} \quad (7b)$$

In our numerical simulations we have assumed the following values of parameters: $m=121[\text{kg}]$, $I_x=3.71[\text{kgm}^2]$, $l=0.121[\text{m}]$, $k_{z0}=175.7[\text{kN/m}]$, $k_{z1}=12.3 \cdot 10^6 [\text{kN/m}^3]$, $c=500 [\text{Ns/m}]$, $L_1=107.2[\text{Nm}]$, $L_2=198.5[\text{Nm}]$, $L_3=82.4[\text{Nm}]$, $L_4=44.5[\text{Nm}]$, $L_5=19.3[\text{Nm}]$, $L_6=12.6[\text{Nm}]$, $\nu_1=1.37[\text{rad}]$, $\nu_2=-0.70[\text{rad}]$, $\nu_3=-0.46[\text{rad}]$, $\nu_4=1.09[\text{rad}]$, $\nu_5=0.50[\text{rad}]$, $\nu_6=0.00[\text{rad}]$. The

amplitudes of excitation are characteristic of the horizontal flight of the aeroplane.

Equations (6a,b) and (7a,b) describe the two-degree-of-freedom, nonautonomous, dynamical system which is defined in the four-dimensional phase space.

3. Stability and chaos analysis.

The model's stability has been additionally verified by applying various excitations: heavyside impulses, white noise and harmonic excitation. The investigation of independent, horizontal displacement described by equation (3) has not revealed any instability. Two remaining, coupled movements have been studied with the help of the Simulink model (Figure 3). It has been observed that the linear version of this model is stable.

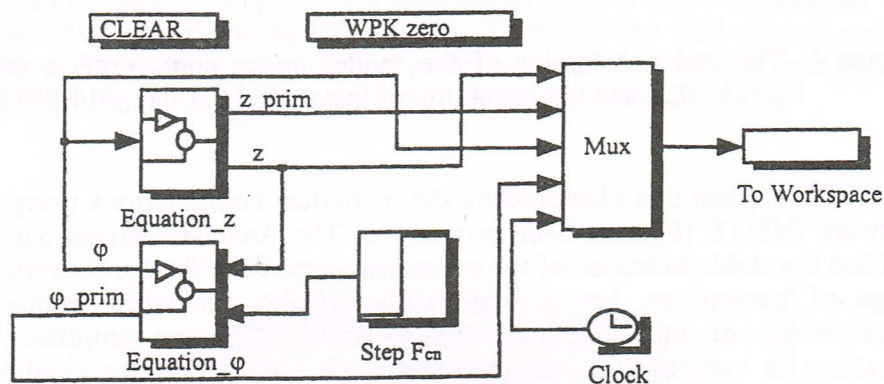


Figure 3. The scheme of the four-dimensional Simulink model (coupled displacement z and rotation ϕ)

When nonlinear stiffness was added, the model was repeatedly losing its stability with a small increase in the input value (from 11,7922 to 11.7923 of dimensionless torque value) – Figure 4.

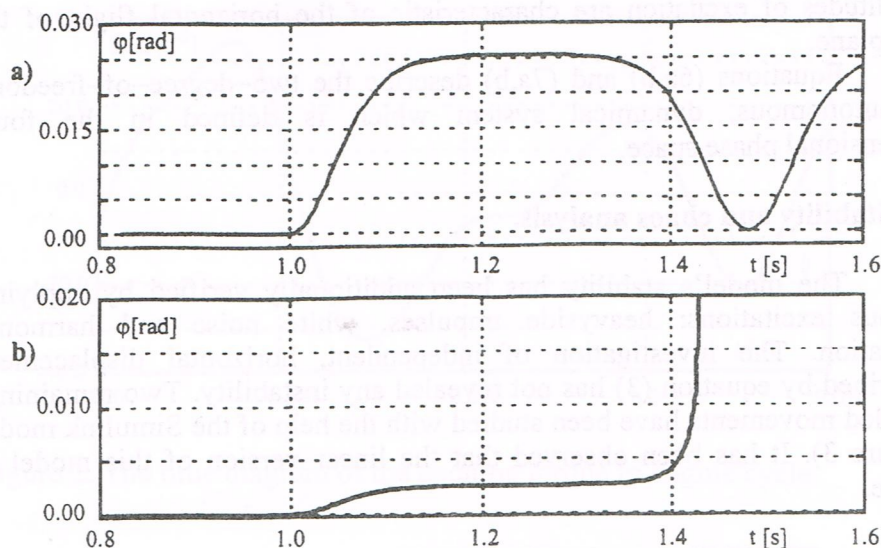


Figure 4. The stable behavior of the model under consideration (a) – $F_{cn}=11.7922$ and the instability of this model (b) – $F_{cn}=11.7923$.

To explain this phenomenon the numerical computations using the software INSITE [8] have been carried out. The Analysis carried out has verified the stable behavior of the examined suspension for the operational range of parameters. For a large value of the excitation frequency characteristic of the horizontal flight ($\omega=262[s^{-1}]$), the amplitude of vibrations is very small – about 10^{-4} [m]. It causes that the nonlinear coupling between equations (1) and (2) disappears and we have two separated systems described by linear equations. We can get the periodic solution of these equations using analytical methods.

However, for a smaller value of the excitation frequency ($\omega<25[s^{-1}]$) and a smaller value of the linear stiffness rate ($k_{z0}=20[kN/m]$), a very big increase in the deformations (amplitude of vibrations), unreal from the functional point of view has been found. It leads to the appearance of the nonlinear coupling (negative feedback) between the equations under consideration.

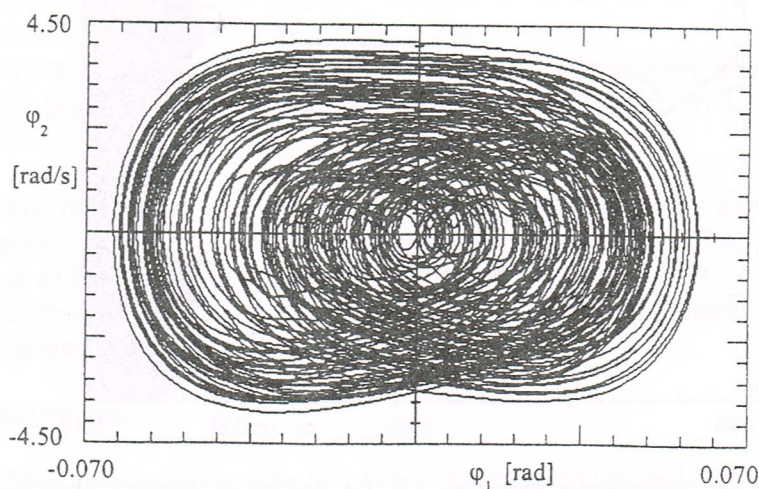
To find out the chaotic responses of the model to multidimensional excitation, the following methods of dynamics investigation have been applied:

- Time diagrams,
- Phase portraits,
- Poincaré maps,
- Bifurcation diagrams,
- Lyapunov exponents.

The numerical simulations of this two-degree-of-freedom, nonlinear system demonstrate various chaotic behaviors. The phase portrait and the Poincaré map in Figure 5 show us the chaotic solution of the analysed system. Randomly distributed points of the Poincaré map are characteristic of a strange chaotic attractor. Also the bifurcation diagrams shown in Figures 6 and 7 have a fractal structure which is typical of chaos.

These bifurcation diagrams have been calculated and drawn as a function of the control parameter ω . First of them (Figure 6) presents the cascade of period doubling bifurcations. It's one of the well-known routes to chaos. An increase in the control parameter causes a series of next period doubling bifurcations and the period of vibrations goes to infinity.

a)



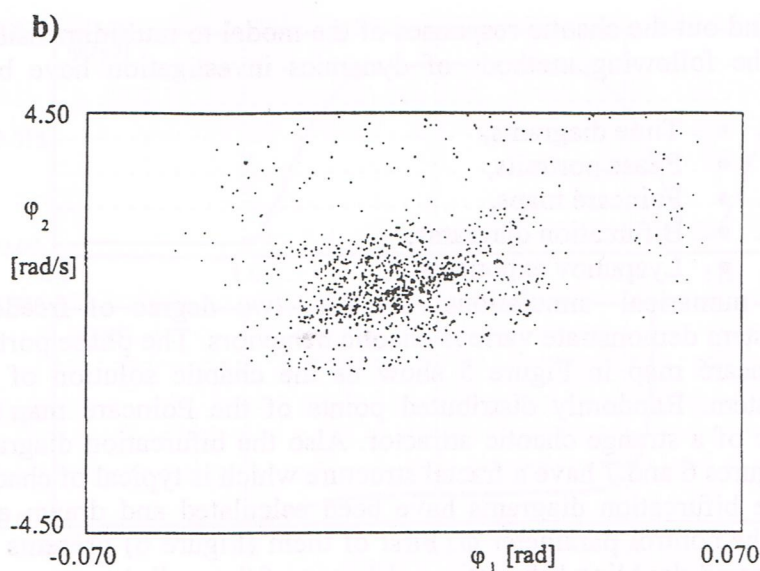


Figure 5. The phase portrait (a) and the Poincaré map (b) of the analysed system; $k_{z0}=20.0$ [kN/m], $k_{z1}=20.0 \cdot 10^6$ [kN/m³], $\omega=13$ [s⁻²].

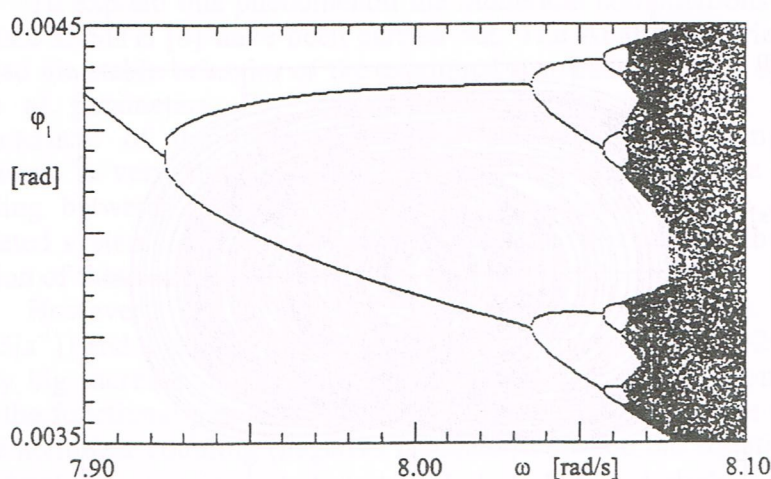


Figure 6. The bifurcation diagram of the analysed system showing the „cascade of period doubling”; $k_{z0}=20.0$ [kN/m], $k_{z1}=20.0 \cdot 10^6$ [kN/m³].

Another route to chaos, called the „break of torus”, is connected with a series of Hopf bifurcations. We can see (Figure 7) that, as a result of the first Hopf bifurcation, the quasi-periodic solution (torus) is generated from the limit cycle (for $\omega=16.465[\text{s}^{-1}]$). After the next Hopf bifurcation the torus loses its stability and a strange chaotic attractor appears (left side of Figure 7).

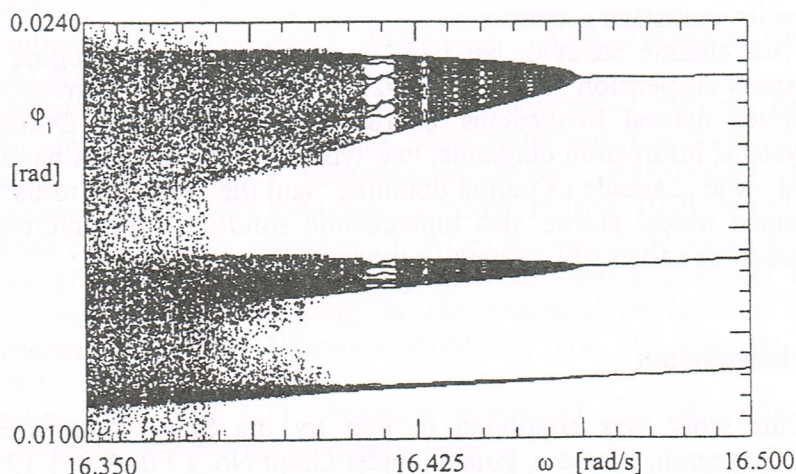


Figure 7. The bifurcation diagram of the analysed system showing the „break of torus”; $k_{z0}=20.0[\text{kN/m}]$, $k_{z1}=20.0 \cdot 10^6 [\text{kN/m}^3]$.

For the system shown in Figure 5 the set of Lyapunov exponents is as follows: $\lambda_1=4.868$, $\lambda_2=1.530$, $\lambda_3=-4.077$, $\lambda_4=-8.426$. The presented spectrum of Lyapunov exponents contains two positive values. It allows us to expect that the system under consideration has a hyperchaotic solution [4] for chosen values of system parameters.

4. Conclusions.

The dynamical analysis of the suspension model allows us to formulate the following conclusions:

1. Model elaborated by means of classical methods of dynamics and identified for a piston Franklin-4 aeroengine powering the light PZL-110 Koliber aeroplane has been verified by comparison of acceleration RMS values obtained with experimental and simulation methods.
2. The simulated behavior of the plane, nonlinear suspension model has shown instability only for very big, unrealistic deformations.
3. In the aeroengine operation range, the model exhibits a limit cycle of a very small amplitude; here the model natural frequencies are distinctly below its excitation spectrum.
4. The rich chaotic behavior has been observed during low engine RPM and small suspension stiffness ($k_{z0}=20[\text{kN/m}]$), with the corresponding linearized natural frequencies: $\omega=18.1[\text{s}^{-1}]$, $\omega=12.56[\text{s}^{-1}]$. During the analysis of bifurcation diagrams, two typical routes to chaos have been found – the „cascade of period doubling” and the „break of torus”. The examined model shows also hiperchaotic solutions, characterized by two positive values of Lyapunov exponents.

Acknowledgements

This work was supported in part by the State Committee for Scientific Research, Warsaw, Poland, under Grant No. 2 P03A 041 12.

References

1. Carr H.R. et al, *A Joint on the Computerisation of In-field Aeroengine Vibration Diagnosis*, Symposium on Propulsion and Energetics, Quebec City, Canada, 1988.
2. Jeż M., *Numerical Simulation of Aeroengine Rubber Constraints*, Nonlinear Vibration Problems, Vol. 25, p. 159–171, Warsaw, Poland, 1993.
3. Kapitaniak T., Wojewoda J., *Bifurkacje i chaos*, Technical University Publishers, Łódź, Poland, 1994 (in Polish).
4. Kapitaniak T., *Chaotic oscillations in mechanical systems*, Nonlinear Science—theory and applications, Manchester and New York, 1991.
5. Kowal J., *Aktywne i semiaktywne metody wibroizolacji układów mechanicznych*, AGH Publishers, Cracow, Poland, 1980 (in Polish).
6. Moon F.C., *Chaotic vibrations*, J. Wiley & Sons, New York, 1987.
7. Osiecki J., *The construction of discrete vibrating model and the existence of weak coupling in the practical analysis of machine dynamics*, Nonlinear Vibration Problems, Vol. 10, Warsaw, Poland, 1969.
8. Parker T.S., Chua L.O., *Practical numerical algorithms for chaotic systems*, Springer-Verlag, Berlin, 1989.
9. Schuster H.G., *Chaos deterministyczny. Wprowadzenie*, State Scientific Publishers, Warsaw, 1995 (in Polish).
10. Swanson D.A., Miller L.R., Norris M.A., *Multidimensional Mount Effectiveness for Vibration Isolation*, Journal of Aircraft, Vol. 31, No. 1, p.188–196, 1994.